Blocking and transmission of traveling flow-distributed-oscillation waves in an absolutely unstable flowing medium

Patrick N. McGraw and Michael Menzinger
Department of Chemistry, University of Toronto, Toronto, Ontario, Canada M5S 3H6
(Received 22 December 2011; published 17 August 2012)

For a flowing, self-oscillating medium, we study the competition between traveling flow-distributed-oscillation waves excited by periodic driving at the upstream boundary and bulk oscillations originating downstream from the boundary. As previously observed in the case of stationary driving, we find that there is a region in parameter space where boundary-driven traveling waves of sufficiently high amplitude can impose themselves on the entire medium despite the presence of an absolute instability, which otherwise tends to block information from upstream. For sufficiently low flow rates, however, the imposed waves are arrested at a nonlinear blocking transition. Unlike the stationary case, we find that the region of imposed waves extends well into regions where, according to the linear approximation, there should be no traveling waves at all. This suggests that the extinction of the traveling waves is analogous to a subcritical Hopf bifurcation.

DOI: 10.1103/PhysRevE.86.026208 PACS number(s): 82.40.Bj, 82.40.Ck, 47.54.Fj

I. INTRODUCTION

The flow-distributed-oscillation (FDO) mechanism of pattern formation can occur in a flowing chemical medium with a Hopf instability (i.e., subject to self-sustaining oscillations) [1–3]. Unlike other pattern-forming mechanisms such as the Turing mechanism [4] and differential-flow instability [5], FDO does not require different rates of transport for different chemical species. Instead, it requires self-sustaining oscillations whose phase can be controlled at the upstream boundary, causing the limit cycle to be spatially distributed as the initial phase recurs at periodic positions downstream.[1] FDO can also occur in a medium that grows by addition at a moving boundary, and in this guise it may constitute a mechanism [9,10] for the gene-expression waves leading to the formation of somites (precursors of vertebrae) in growing vertebrate embryos [11,12].

A distinctive feature of FDO is that it allows patterns to be controlled by manipulating the upstream boundary condition. A stationary boundary condition results in stationary waves, while oscillatory driving can generate traveling waves which travel downstream if the driving is faster than the natural oscillation frequency of the medium and upstream otherwise [9,10,13]. If the driving frequency is identical to the natural frequency, then the Hopf mode, i.e., synchronous oscillation throughout the medium, is excited [14]. It is this Hopf mode which always has the largest spatial growth rate [15]. In general, the existence of FDO depends on the flow velocity v by way of the ratio D/v^2, where D is the diffusion constant [15]. FDO waves become evanescent (spatially decaying) when the flow velocity falls below a threshold.

In a flowing medium, an instability may be either convective or absolute. In the first case, perturbations grow in the frame of reference which moves with the fluid, but are advected downstream so that at any fixed position they decay. Absolute instability, on the other hand, means that disturbances may propagate upstream as well as downstream and can therefore grow at a fixed position [1,16,17]. If the underlying Hopf instability that makes FDO possible is absolute, then this raises the possibility that oscillations originating downstream in the bulk of the medium can not only persist but propagate upstream so as to compete with FDO waves that are driven by the upstream boundary. For this reason, FDO has usually been studied under convectively unstable circumstances—this allows the upstream boundary condition to fully control the pattern formation in the rest of the medium, while any disturbances that originate farther downstream are eventually advected out of the system. However, Kuptsov [18] has examined numerically and theoretically a more complicated case in which an absolutely unstable medium is driven by constant forcing at the upstream boundary. In this case, there is direct nonlinear competition between uniform bulk oscillations originating downstream and stationary waves driven by the boundary. Penetration of the stationary waves may then be amplitude-dependent—a sufficiently strong perturbation at the boundary can push the Hopf oscillations away despite their tendency to propagate upstream.

The current paper extends the previous work [18] by examining the effect of periodic (rather than steady) driving on an absolutely unstable medium. Periodic driving in the convectively unstable case leads to traveling waves. As in the case of steady forcing and stationary waves, we find for periodic driving that there is a regime of nonlinear competition between the traveling waves originating at the boundary and the absolutely unstable Hopf mode. As with stationary waves, we find that there is a portion of parameter space where the penetration of the traveling wave signal into the medium is amplitude-dependent. We also find a threshold flow velocity below which the transmission of traveling waves is blocked regardless of the driving amplitude.

Unlike the stationary-wave case, however, we find that traveling waves may still exist and be able to penetrate into the medium even at velocities well below the threshold where a linear approximation predicts that the waves should

[1] A closely related phenomenon which does include the possibility of differential transport is referred to in some works as flow and diffusion distributed structures (FDS). This more general case can also lead to structures controlled by the boundary [6] and interactions among different types of waves [7]. The relationship between the cases with and without differential flow or diffusion is also discussed in [8]. Here, we only consider cases without differential transport.

be extinguished (evanescent). This suggests that under these circumstances, the evanescence bifurcation for traveling waves is subcritical. We observe that there are in general two types of domain boundaries (DBs) separating the traveling waves from the uniform (Hopf) oscillations, which we call smooth and rough DBs. Smooth DBs in general propagate much more rapidly, and a DB may change rather abruptly from one type to the other as the driving amplitude or flow velocity is altered.

In general, the FDO mechanism has been studied more extensively in the case of stationary driving than periodic driving. Among our motivations for examining periodic driving more closely is the biological application of FDO as a mechanism for the gene-expression waves involved in somitogenesis. A candidate scenario for the regulation of somitogenesis involves a cellular oscillator, the segmentation clock [11,12], whose frequency decreases with downstream distance (i.e., away from the moving growth boundary of the embryo) but which is driven by the faster oscillations at the tip [9,10]. The mechanism by which embryos arrest the formation of somites and thus achieve a fixed, species-specific number of segments remains open to debate [19,20]. We speculate that the dynamical blocking of waves described in this paper may be the key to this mechanism. With this in mind, we focus mainly on the case in which the driving is at a frequency higher than the natural oscillation frequency, which also presents somewhat fewer complications than the other case with driving below the natural frequency. (Specifically, in the latter case, the effects we consider here compete with resonant breakup of the type described in [21] in a way that is hard to disentangle in numerical experiments.)

In the following section, we review briefly the behavior of traveling and stationary waves and the types of bifurcations that separate different regimes of wave behavior. Then in Sec. III, we illustrate these different behaviors with space-time plots for a model reaction-diffusion-advection system. We show qualitatively the meaning of the two linear thresholds (absolute instability and evanescence) for the behavior of the Hopf and FDO modes, and then we show how a third distinct threshold (the blocking transition) comes into play when there is nonlinear competition between modes. Section IV discusses types of domain boundaries that arise in this nonlinear competition. Finally, in Sec. V we present and discuss numerical measurements of blocking thresholds, i.e., the threshold velocities at which waves of several different frequencies are blocked by the Hopf oscillations. This is followed by some concluding remarks.

II. EVANESCENCE AND ABSOLUTE INSTABILITY THRESHOLDS FOR THE FDO SYSTEM

The FDO mechanism generically occurs in a system described by the reaction-diffusion-advection (RDA) equation

$$\frac{\partial \mathbf{U}}{\partial t} = \mathbf{f}(\mathbf{U};C) - v\frac{\partial \mathbf{U}}{\partial x} + D\frac{\partial^2 \mathbf{U}}{\partial x^2}, \tag{1}$$

where $\mathbf{U}(x,t)$ is a vector of dynamical variables (concentrations of species), $v > 0$ is the flow velocity, D is the diffusion coefficient, and $\mathbf{f}(\mathbf{U};C)$ is a vector-valued function that encodes the reaction kinetics and may depend on some control parameters C. In the current work, we consider as a simple kinetic model the van der Pol or FitzHugh-Nagumo [22] system,

$$\frac{\partial U}{\partial t} = E(U - U^3 - W), \quad \frac{\partial W}{\partial t} = -U + AW + B. \tag{2}$$

Although not chemically realistic (unlike chemical concentrations, the variables can be negative), this model has been used frequently as a toy model in studies of chemical pattern formation because it has many of the essential features of more directly chemically inspired oscillator models such as the Lengyel-Epstein [23], Brusselator [24], and Oregonator [25] models while being simpler to analyze and understand. The parameters A and B can be tuned to allow bistability or excitable behavior if $A < 1$ or $B \neq 0$. In the current work, we take $A = 10$ and $B = 0$, which allows only oscillatory or monostable dynamics, while allowing E to vary as the single control parameter. For all $A > 1$, the model undergoes a supercritical Hopf bifurcation at $E = 1$ and has a stable limit cycle for $E > 1$. With increasing E, two separate time scales develop, the oscillations become less nearly sinusoidal, and the nonlinearity becomes stronger [15]. Without loss of generality, we also set $D = 1$ because a change in the diffusion constant can be absorbed into a rescaling of units together with the velocity. As discussed elsewhere [15], only the ratio D/v^2 is dynamically important. In experiments, v is easier to manipulate than D, so it is usually taken as the control parameter.

The starting point for the analysis of wavelike disturbances in the medium described by (1) is the dispersion relation, obtained by substituting the ansatz

$$\mathbf{U} = \mathbf{U}_0 + \mathbf{A}\exp[i(\omega t - kx)] \tag{3}$$

into the RDA equation (1), where $\mathbf{U}_0$ is a (generally unstable) equilibrium point of the kinetics, i.e., $\mathbf{f}(\mathbf{U}_0;C) = 0$, and the frequency ω and wave number k may be complex. As shown in [15], the dispersion relation can be reduced to

$$i\omega = \alpha + i\beta + ivk - Dk^2, \tag{4}$$

where $\lambda = \alpha + i\beta$ is the (complex) eigenvalue of the Jabobian matrix $\partial\mathbf{f}/\partial\mathbf{U}$ evaluated at the equilibrium point. [In our model with kinetics given by Eq. (2), the equilibrium is at the origin of phase space, $(U,W) = (0,0)$.]

To understand the effect of small-amplitude driving at the boundary, one is interested in solutions to the dispersion relation that match the upstream boundary condition, which is taken to be an oscillatory function with steady amplitude. This therefore involves solving (4) for k, using $\omega = \omega_D$ (where ω_D is the driving frequency) as the independent variable. Stationary waves correspond to the most frequently studied case $\omega = 0$. $k(\omega)$ is in general complex. $\mathrm{Im}\,k > 0$ implies that a small-amplitude disturbance at the boundary creates a wave that grows with downstream distance (and, in general, matches up with a nonlinear wave with saturated amplitude). $\mathrm{Im}\,k < 0$, on the other hand, implies an *evanescent wave*, one that decays with downstream distance and therefore fails to establish itself throughout the medium. Typically, $\mathrm{Im}\,k$ increases with increasing velocity. As noted above, decreasing v is equivalent to increasing the diffusion in the ratio D/v^2, and thus waves with nonzero wave number are increasingly damped as v decreases.

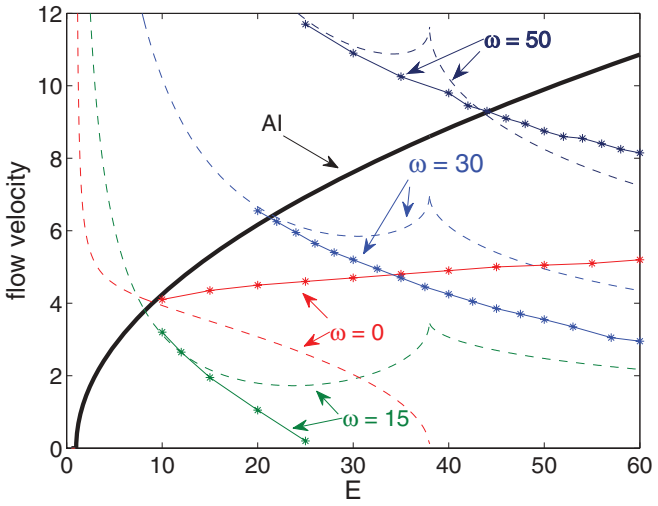

FIG. 1. (Color online) Three types of threshold velocities as functions of control parameter E. Thick solid line: absolute instability (AI) threshold. Dotted lines: evanescence thresholds (based on linearization about the unstable equilibrium) for waves at several indicated frequencies. Solid lines with data points: thresholds for the blocking (see Sec. V) of boundary-driven waves, obtained numerically.

The group velocity $d\omega/dk$ can also be obtained by solving the dispersion relation. If $d\omega/dk > 0$ for all modes, which is generically true for large enough v, then the system is convectively unstable, as no disturbances propagate upstream and even a disturbance that grows with downstream distance is advected away and therefore does not grow at a fixed position. The system, on the other hand, becomes *absolutely unstable* when the flow velocity is reduced below the intrinsic spreading velocity of disturbances. In this case, the group velocity is negative for some modes, meaning that some disturbances can travel upstream and the system's asymptotic behavior is no longer controlled exclusively by the upstream boundary condition. The mode with $\mathrm{Re}\, k = 0$, $\omega = \beta$, corresponding to uniform oscillations (also called the Hopf mode), always has the highest spatial growth rate and is also the first to cross the threshold from positive to negative group velocity.

In Fig. 1 (which is discussed more fully in Sec. V), we plot these threshold velocities for absolute instability and for the transitions to evanescence of waves at several different frequencies, as functions of the control parameter E in the model (2). The shapes of these curves as functions of the control parameter show features typical of many other kinetic models [2,26,27]. In particular, as the kinetic system approaches a Hopf bifurcation, at $E = 1$ in this case, the absolute instability threshold vanishes and the evanescence thresholds approach infinity. This is because for parameter values below the Hopf bifurcation, all oscillations are intrinsically damped, even without the effects of diffusion. Another noticeable feature of the curves occurs at $E = 38$, where the imaginary part of the Jacobian eigenvalue vanishes and the unstable equilibrium changes from a focus to a node. The $\omega = 0$ evanescence threshold vanishes at this point (zero-frequency waves can no longer be linearly damped), and the other ($\omega > 0$) threshold curves exhibit cusps.

III. QUALITATIVE WAVE BEHAVIOR, NONLINEAR COMPETITION, AND THE BLOCKING THRESHOLD

The absolute instability and evanescence thresholds discussed above govern the linear behaviors of different wave modes. In this section, we illustrate these thresholds qualitatively and then show how nonlinear interaction can arise. This will lead us to describe a third, nonlinear threshold.

To illustrate the three thresholds under discussion, we present some space-time plots (Figs. 2 and 3) of numerical solutions of the RDA equation (1) showing the behavior of FDO waves and Hopf oscillations in several different regions of parameter space. In these plots, the gray level represents the value of U in the kinetic model (2). Since we are most interested in the competition between bulk oscillations and boundary-driven waves, all numerical integrations use uniform initial conditions in order to set up bulk Hopf oscillations, while the upstream boundary conditions are varied. The left column of plots in Fig. 2 illustrates the meaning of the absolute

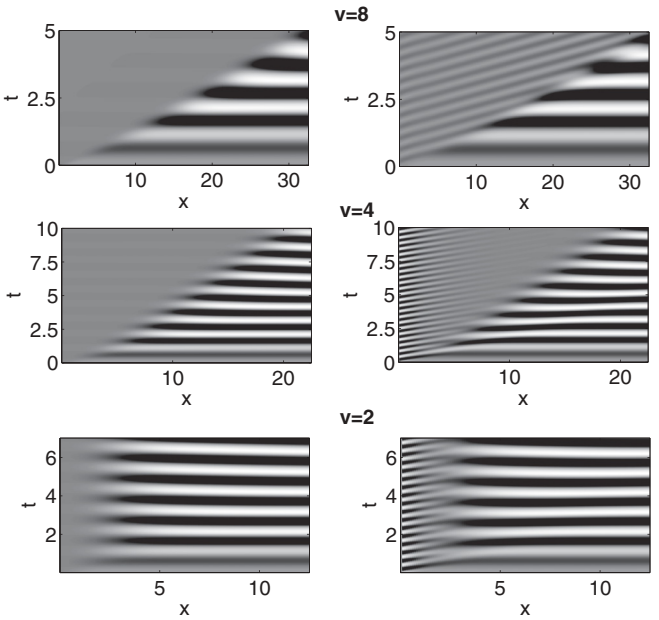

FIG. 2. Space-time plots at three different flow velocities, illustrating the evanescence threshold (for a traveling wave) and the absolute instability threshold. In the left column of plots, there is no driving at the upstream boundary (i.e., the boundary condition is held at the equilibrium point), whereas in the right column, there is oscillatory driving at a frequency higher than the natural oscillation frequency, which tends to produce downstream traveling waves. At sufficiently high flow rate (top row), the traveling waves are sustained and fill the entire system. Below some threshold velocity, however, the traveling waves are evanescent; i.e., they decay with downstream distance. On the other hand, the uniform oscillations set up by the initial conditions are advected downstream and out of the system. At a still lower velocity, the uniform oscillations are no longer advected out of the system but fill the entire system except for a boundary of fixed thickness near the inflow. Comparison of the left column with the right column suggests that the uniform oscillations and the boundary-driven traveling waves do not significantly affect each other. Axes are measured in units of the model equation (2), and the gray level represents the variable U (more precisely, it is proportional to the positive number $U + 2$) in that model.

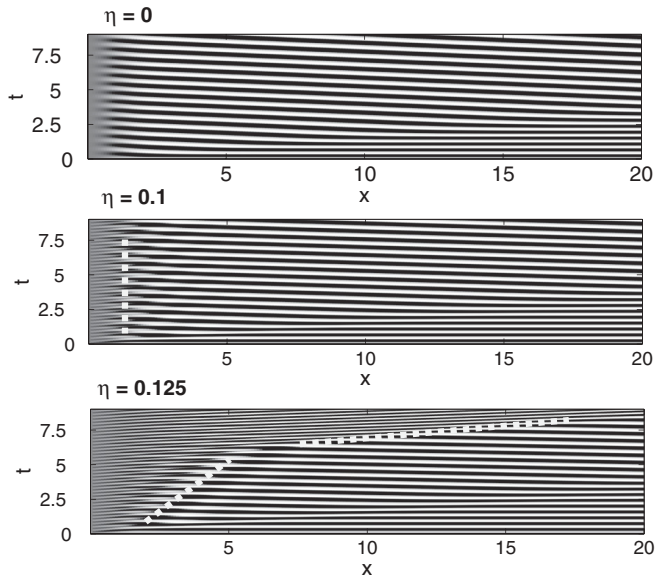

FIG. 3. Interaction between boundary-driven traveling waves and Hopf oscillations in the case $\omega = 27, E = 30, v = 6$, where the evanescence threshold falls below the absolute instability threshold. The top plot, with no driving (zero amplitude driving) at the boundary, shows that the Hopf oscillations are absolutely unstable: they fill the entire system except for a thin boundary layer. When oscillatory driving with an amplitude $\eta = 0.1$ is imposed, the resulting traveling waves are blocked by the Hopf oscillations—they do not propagate beyond the thin boundary layer. When the amplitude is increased to $\eta = 0.125$, however, the traveling waves are able to push the Hopf oscillations away from the boundary and a downstream-moving domain boundary (DB) is formed. The dotted white lines are a guide to the eye showing the approximate trajectories of the DB's that separate traveling waves from Hopf oscillations.

instability (AI) threshold: in the upper two plots, the Hopf instability is convective, and the uniform oscillations which are established by the initial conditions are advected out of the system with time. No disturbances are able to propagate upstream and disturb the equilibrium state. In the bottom plot, the flow velocity is below the AI threshold, and the bulk oscillations therefore can propagate against the flow, so that they fill the whole system except for a thin boundary layer. In the right column, an oscillatory driving

$$\begin{pmatrix} U(t,0) \\ W(t,0) \end{pmatrix} = \eta \begin{pmatrix} \cos \omega_D t \\ \sin \omega_D t \end{pmatrix} \tag{5}$$

with amplitude η and driving frequency ω_D is added at the upstream boundary, and traveling waves are generated. (For $\omega_D > 0$, this boundary condition circulates in phase space in the same direction as the limit cycle, and has a significant overlap with the growing FDO modes; see also Refs. [15] and [8] for discussions of the driving waveform.) At sufficiently high flow velocities, these traveling waves grow to an asymptotically steady amplitude and eventually fill the whole system, once the initial bulk oscillations have been swept away by the flow. At somewhat lower velocities, however (second row), the traveling waves are evanescent rather than growing.

Comparison of the two columns (with and without oscillatory driving) in Fig. 2 shows that the bulk oscillations and traveling waves affect each other very little: the bulk oscillations are either swept downstream or form a thin boundary layer, independently of whether there are traveling waves or not. This is generally true in regions of parameter space where the evanescence transition lies well above the AI transition. A different situation can occur when the AI threshold occurs at a higher flow velocity than the evanescence threshold. This is illustrated in Fig. 3, which shows a series of plots for a flow velocity $v_{ev} < v < v_{AI}$. In this case, there is a direct nonlinear competition between the Hopf oscillations generated by the initial conditions and the traveling waves generated by the upstream driving. In the absence of upstream driving, the system is clearly absolutely unstable. Low-amplitude driving expands the boundary layer slightly, but at a sufficiently high amplitude, the traveling waves can push the Hopf oscillations out of the way and propagate into the whole system. The situation is analogous to what was referred to as "imposed convective instability" in Ref. [18].

IV. SMOOTH AND ROUGH DOMAIN BOUNDARIES

In the bottom plot of Fig. 3, the two types of patterns, Hopf oscillations and traveling waves, are separated by a domain boundary (DB) which moves downstream. A feature which was not seen in the case of stationary waves is that the nature of the DB evidently changes at time $t \approx 6$ from a slow-moving DB to a faster one. At the faster DB, unlike the slower one, the wavefronts of the traveling waves match continuously to the oscillations in the downstream region. The space-time wavefronts are unbroken and simply change their velocity. We refer to this latter type of DB as a "smooth" DB and the other as a "rough" DB. As we will argue below, DB type is necessarily correlated with DB velocity. Smooth DB's generically propagate at speeds close to the flow velocity—i.e., they are approximately comoving with the fluid, whereas rough DB's propagate more slowly. The correlation between DB type and traveling wave amplitude seen here is also generic: small-amplitude waves form slow-moving rough DB's, but as the amplitude of a growing wave increases to saturation, the DB speeds up to an asymptotic velocity that depends on the flow velocity and driving frequency, and may remain rough or become smooth as in Fig. 3. In the particular case depicted in Fig. 3, the type of DB changes quite abruptly. On the other hand, if the driving amplitude is above the saturated amplitude, then the amplitude decreases with downstream distance and the DB correspondingly slows down to its asymptotic velocity rather than speeding up. Further discussion of the dependence of DB type and asymptotic velocity on control parameters is given in Sec. V.

Considering a DB as a junction between two waves, each with its own wave number and frequency, one can derive conditions for the existence of a smooth DB. Let the wave number and frequency of the wave to the left of the DB be ω_1 and k_1, and let those for the other wave be ω_2 and k_2. In the special case of uniform oscillations, $k_2 = 0$. Using the methods described in Ref. [21], under a Galilean transformation the frequency of a wave ω_M as observed in a moving frame of

reference is

$$\omega_M = \omega + kV, \tag{6}$$

where ω and k are the frequency and wave number as defined in the fixed reference frame and V is the velocity of the moving reference frame. ω_M can be interpreted as the frequency measured by a moving observer, or the number of wave crests per second encountered by a trajectory which moves at velocity V. The moving DB can be viewed as a worldline that cuts across both waves (the one to the left and the one to the right). A smooth DB is one which always encounters equal numbers of wavefronts to its left and to its right, so that every wavefront on the right joins smoothly to one on the left. This means that the frequency of both waves is identical, as viewed in the reference frame of the moving DB, which leads to the condition

$$\omega_1 + k_1 V = \omega_2 + k_2 V \tag{7}$$

and thus

$$V = \frac{\omega_1 - \omega_2}{k_2 - k_1}. \tag{8}$$

In the so-called kinematic [28] or low-diffusion limit, the frequency of all phase waves in a frame comoving with the fluid (at flow velocity v) is equal to the intrinsic oscillation frequency ω_0 of the underlying chemical system, so that

$$\omega_0 = \omega_1 + k_1 v = \omega_2 + k_2 v. \tag{9}$$

It is easily shown that Eqs. (9) and (8) together imply $V = v$; in other words, in the kinematic limit a smooth DB necessarily travels at the flow velocity. The rough DB, on the other hand, travels more slowly than the flow velocity. In the one shown in Fig. 3, the DB cuts off several wavefronts of the traveling wave to the left for each oscillation to the right. In other words, we have

$$\omega_{M1} = r\omega_{M2}, \tag{10}$$

where ω_{M1} and ω_{M2} are the frequencies in the DB's frame of reference, and $r > 1$. We are especially interested in DB's that separate an FDO wave on the left (upstream) from uniform oscillations downstream, in which case $k_2 = 0$ and $\omega_2 = \omega_0$. In this case, Eqs. (9), (6), and (10) together lead to the result

$$\frac{V}{v} = \frac{\omega_1 - r\omega_0}{\omega_1 - \omega_0}, \tag{11}$$

where the case $r = 1$ is that of a smooth DB. A stationary DB ($V = 0$), on the other hand, has $r = \omega_1/\omega_0$ as expected, while $0 < V < v$ for the cases

$$1 < r < \frac{\omega_1}{\omega_0}, \quad \omega_1 > \omega_0 \quad \text{or}$$
$$\frac{\omega_1}{\omega_0} < r < 1, \quad \omega_1 < \omega_0.$$

We note that the result (11) is not exact, since it is based on two approximations, the first being the kinematic limit (and that all waveforms have the same frequency in the comoving frame of the fluid) and the second being the assumption that $k_2 = 0$ for the medium immediately to the right (downstream) of the DB. In fact, if one looks closely at the plots in Fig. 3, one can see that the initial uniform oscillations adjust slightly in response to the presence of an upstream boundary even in the absence of driving, so that they are no longer precisely uniformly synchronized but instead have a gentle phase gradient and thus a nonzero wave number.

V. MEASURED THRESHOLDS FOR BLOCKING/TRANSMISSION, AND SUBCRITICALITY OF THE EVANESCENCE TRANSITION

As explained above, imposed convective instability means that a traveling (or stationary) FDO wave of sufficiently high amplitude generated by driving at the upstream boundary can establish itself and propagate downstream despite the presence of an absolute instability. As in the previously studied case of stationary driving, likewise for oscillatory driving the imposed convective instability occurs between the AI threshold and some lower threshold velocity at which the DB between the boundary-driven waves and the Hopf oscillations becomes stationary. Kupstov [18] describes the region below this threshold as one of "coexistence" (meaning that the two types of patterns coexist on opposite sides of a stationary DB). We refer to this transition as the *blocking threshold*, because above it, the FDO waves generated by the boundary are transmitted asymptotically far downstream, while below it those boundary-driven waves are blocked and only penetrate a finite distance into the medium, regardless of the driving amplitude.

In this section, we present our numerical results on the blocking thresholds as functions of the control parameter E for FDO waves in our model at several different frequencies ω. We estimated this threshold by performing a series of numerical integrations at different flow velocities while holding other parameters fixed, and by examining the space-time plots. We imposed an oscillatory driving of the form of Eq. (5) with amplitude $\eta = 2$, significantly larger than the amplitude of the natural limit cycle. Our reasoning was that if such a large amplitude signal was blocked, then all traveling waves at that frequency would certainly be blocked. In most cases, we found that the transition was rather sharp; a small change of the flow velocity would cause the DB velocity to change abruptly from positive (downstream) to zero. An example of such an abrupt transition is shown in the space-time plots of Fig. 4. In a few cases, the transition was a bit harder to detect because the DB took a significant amount of time to reach an asymptotic velocity, and in those cases it was difficult to determine whether the asymptotic velocity was truly zero or merely slow but nonzero. We estimate an uncertainty in the velocity threshold of at most ± 0.1 space units/time unit. The results for the thresholds are plotted in Fig. 1, which also shows the AI threshold and the evanescence thresholds as predicted by solving the dispersion relation (4).

A particularly interesting feature of the results is that, with the exception of the $\omega = 0$ case, the blocking thresholds actually fall *below* the evanescence thresholds within a substantial range of E values. While surprising, this is not logically inconsistent, since the evanescence thresholds are derived from a dispersion relation that describes *small-amplitude* perturbations of the unstable equilibrium. These results suggest that the evanescence transition can be subcritical; small-amplitude waves decay, but large-amplitude ones are stable. A subcritical evanescence transition was noted [26] for stationary waves in

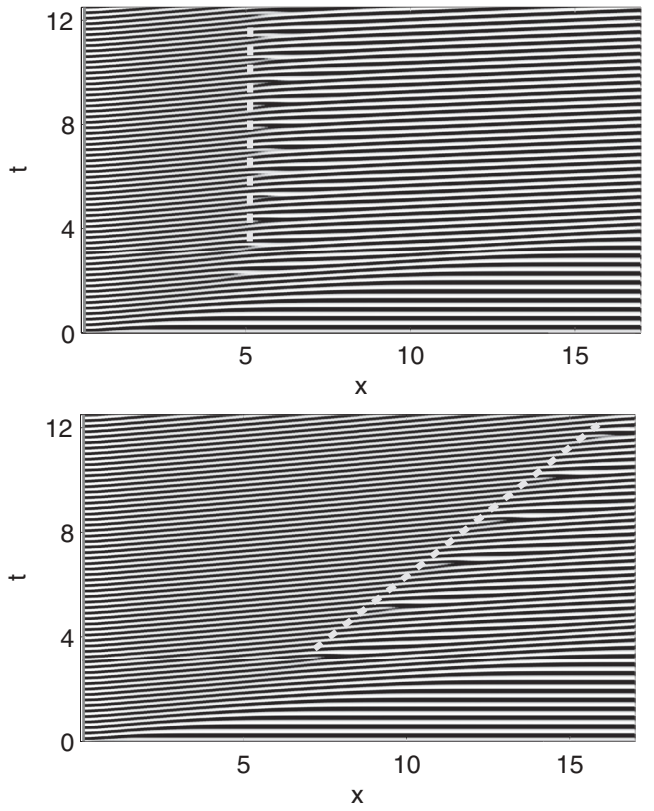

FIG. 4. Numerical detection of the blocking threshold. Here $E = 57$, and the upstream boundary is driven at $\omega = 30$. In both plots, a DB marks the limit of penetration of the waves under control of the upstream boundary. (White lines show the approximate location of the DB.) In the upper plot, the flow velocity is $v = 3.0$. After a transient, the DB comes to rest—the boundary-driven waves are blocked. In the lower plot, $v = 3.1$, and the DB abruptly changes to a downstream-moving one, with a DB velocity of approximately 1.25. We conclude that the blocking threshold in this case is $v_B = 3.05 \pm 0.05$.

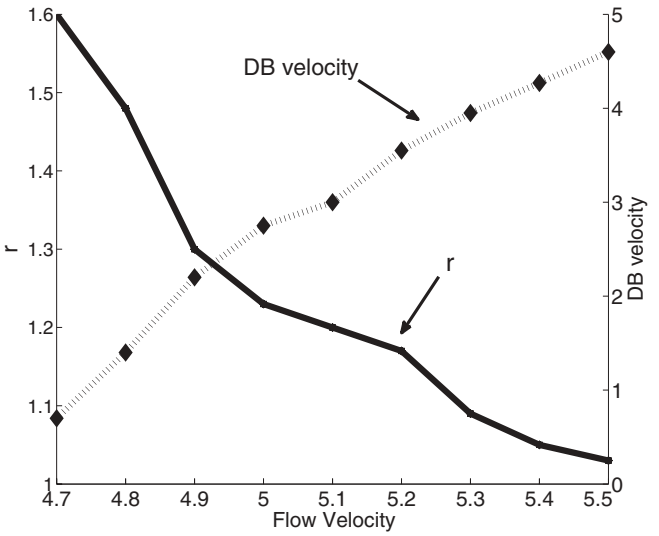

FIG. 5. Roughness ratio r and domain boundary velocity V_{DB} as functions of the flow velocity v, for $E = 35$ and $\omega = 30$. $v = 4.7$ lies just above the blocking threshold—the DB velocity drops to zero below this point. As the flow velocity increases, the DB speed increases rapidly and the ratio r [as defined in Eq. (10)] decreases toward unity.

the chlorine dioxide-iodine-malonic-acid (CDIMA) reaction, in that case without absolute instability. In most of the cases we examined, the blocking thresholds join the linear evanescence curves near the points where the latter cross the AI boundary, so that the region of subcriticality lies inside the AI region. An exception is the high-frequency driving case $\omega_D = 50$. In the vicinity of the cusp of the evanescence curve, we also found propagating FDO waves at velocities below the linear threshold (but above the AI threshold). These persist down to a threshold velocity which we have plotted in Fig. 1 as an extension of the blocking threshold curve (the extended curve represents in any case the bifurcation locus above which boundary-driven traveling waves can propagate fully into the medium, and below which they cannot). Below this threshold, the high-amplitude traveling waves do not decay smoothly but instead break up into a different, irregular traveling wave pattern of lower frequency. The dynamics of waves at such high driving frequency (by comparison, the frequency of the underlying kinetic model's limit cycle at $E = 38$ is 15) is only incompletely studied and is a subject for future work. We also examined the change from a rough to a smooth domain boundary for only a few values of E and ω. For this study, we again used a high-amplitude driving, and for a series of velocities above the blocking threshold we examined the downstream-moving DB. For flow velocities just above threshold, the DB was a slow-moving rough DB with the ratio $r > 1$ as defined in Eq. (10). As the flow velocity increased, so did the DB velocity, while r decreased until it reached unity and a smooth DB was formed. The dependence of r and the DB velocity is plotted in Fig. 5 for the parameters $E = 35$ and $\omega = 30$. To clarify the relationships of the phenomena under discussion, we now summarize the transitions in traveling wave behavior that generically occur as the flow velocity is decreased in the case in which the AI threshold lies above the evanescence threshold. Above the AI threshold, traveling waves controlled by the upstream boundary propagate freely into the medium without interference from the Hopf mode. Immediately below the AI threshold, penetration of traveling waves becomes amplitude-dependent. In this range, perturbations above a threshold amplitude propagate into the medium despite the absolutely unstable mode (forming a smooth DB moving asymptotically with a fixed downstream velocity), while low-amplitude waves are blocked and instead form a stationary DB with the Hopf oscillations. As v decreases further, the amplitude threshold increases from zero at the AI threshold and approaches the saturated amplitude of the traveling waves. At still lower v, the asymptotic DB changes from smooth to rough but still moves downstream. At a still lower v (namely the blocking threshold), the DB becomes asymptotically stationary and traveling waves fail to penetrate beyond a finite distance, regardless of the perturbation amplitude. In the present work, we have mapped the blocking thresholds in some detail, but we have investigated the change of DB type only for a few parameter values.

VI. CONCLUSIONS

Following up on the discussion of imposed convective instability in Ref. [18], we have studied the corresponding phenomenon for traveling waves driven by oscillatory boundary conditions at the inlet of a reaction-diffusion-advection system. It has already been widely noted that a convectively unstable system is an arena in which pattern formation throughout the system can be placed under the control of the upstream boundary condition, which may be stationary, oscillating, or noisy in the case of noise-sustained structures [17]. The current work together with that of [18] shows that under the right conditions, the boundary can drive pattern formation despite the existence of an absolute instability, which, in principle, allows disturbances to travel upstream as well as downstream. The penetration of the boundary-driven pattern into the system is limited by a domain boundary which separates regions of two different wave patterns, and the behavior of that DB depends on a nonlinear and amplitude-dependent competition between the two patterns. We also examined the nature of the DB itself, which may either be rough or smooth. We noted that in general, rough DB's move slower than the flow velocity while smooth DB's move much closer to the flow velocity. In some cases, the transition from a rough to a smooth DB can be quite abrupt. Smooth DB's were not observed in the case of stationary waves. Another novel feature unique to traveling waves is that the threshold for blocking can lie significantly below the (linear, small-amplitude) evanescence threshold. In other words, large-amplitude traveling waves at some frequencies can be maintained and even push the absolutely unstable Hopf oscillations out of their way, despite the fact that a linear analysis predicts that those waves should decay. This suggests that the transition to damped (evanescent) waves can be subcritical.

Since the segmentation (somitogenesis) of embryos is driven by an oscillation at the growing tip of the embryo (equivalent, via a Galilean transformation, to the upstream boundary of a flow system), and the exact kinetics of this oscillator are largely unknown, it is useful to gain further understanding of the circumstances under which information (in the form of an imposed pattern) is transmitted from the boundary and when the transmission is blocked. One of our chief motivations for this study is the possibility that somitogenesis stops when the growth rate slows such that a blocking threshold is crossed.

ACKNOWLEDGMENTS

This work was supported by the NSERC of Canada.

[1] S. P. Kuznetsov, E. Mosekilde, G. Dewel, and P. Borckmans, J. Chem. Phys. **106**, 7609 (1997).
[2] P. Andrésen, M. Bache, E. Mosekilde, G. Dewel, and P. Borckmanns, Phys. Rev. E **60**, 297 (1999).
[3] M. Kærn and M. Menzinger, Phys. Rev. E **60**, R3471 (1999).
[4] A. M. Turing, Philos. Trans. R. Soc. London, Ser. B **237**, 37 (1952).
[5] A. B. Rovinsky and M. Menzinger, Phys. Rev. Lett. **69**, 1193 (1992).
[6] R. A. Satnoianu and M. Menzinger, Phys. Rev. E **62**, 113 (2000).
[7] R. A. Satnoianu, Phys. Rev. E **68**, 032101 (2003).
[8] P. N. McGraw and M. Menzinger, Phys. Rev. E **72**, 026210 (2005).
[9] M. Kærn, M. Menzinger, and A. Hunding, J. Theor. Biol. **207**, 473 (2000).
[10] M. Kærn, M. Menzinger, R. Satnoianu, and A. Hunding, Faraday Discuss. **120**, 295 (2002).
[11] O. Pourquié, Annu. Rev. Cell Dev. Biol. **17**, 311 (2001).
[12] O. Pourquié, Science **301**, 328 (2003).
[13] M. Kærn, D. G. Miguez, A. P. Muñuzuri, and M. Menzinger, Biophys. Chem. **110**, 231 (2004).
[14] M. Kærn and M. Menzinger, J. Phys. Chem. A **106**, 4897 (2002).
[15] P. N. McGraw and M. Menzinger, Phys. Rev. E **68**, 066122 (2003).
[16] R. J. Briggs, *Electron Stream Interactions with Plasmas* (MIT Press, Cambridge, MA, 1964).
[17] R. J. Deissler, J. Stat. Phys. **40**, 371 (1985); **54**, 1459 (1989).
[18] P. V. Kuptsov, Physica D **197**, 174 (2004).
[19] E. M. Özbudak and O. Pourquié, Curr. Opin. Genet. Devel. **18**, 317 (2008); C. Gomez *et al*., Nature (London) **454**, 335 (2008); M.-L. Dequéant and O. Pourquié, Nature Rev. Genet. **5**, 370 (2008).
[20] C. Gomez *et al*., Nature (London) **454**, 335 (2008); C. Gomez and O. Pourquié, J. Exp. Zool. **312B**, 533 (2009).
[21] P. N. McGraw, M. Menzinger, and A. P. Munuzuri, Phys. Rev. E **80**, 026209 (2009).
[22] J. S. Nagumo, S. Arimoto, and S. Yoshizawa, Proc. IRE **50**, 2061 (1962); R. FitzHugh, Biophys. J. **1**, 445 (1961).
[23] I. Lengyel, G. Rabai, and I. R. Epstein, J. Am. Chem. Soc. **112**, 9104 (1990).
[24] G. Nicolis and I. Prigogine, Self-Organization in Nonequilibrium Systems (Wiley, New York, 1977); P. Glansdorf and I. Prigogine, *Thermodynamic Theory of Structure, Stability and Fluctuations* (Interscience, New York, 1971).
[25] J. J. Tyson, in *Oscillations and Travelling Waves in Chemical Systems*, edited by R. Field and M. Burger (Wiley, New York, 1985), pp. 93–144.
[26] J. R. Bamforth, S. Kalliadasis, J. H. Merkin, and S. K. Scott, Phys. Chem. Chem. Phys. **2**, 4013 (2000).
[27] J. R. Bamforth, J. H. Merkin, S. K. Scott, R. Toth, and V. Gaspar, Phys. Chem. Chem. Phys. **3**, 1435 (2001).
[28] P. Andrésen, E. Mosekilde, G. Dewel, and P. Borckmans, Phys. Rev. E **62**, 2992 (2000); M. Kærn and M. Menzinger, *ibid*. **62**, 2994 (2000).